


General Theory for Bilayer Stacking Ferroelectricity

Junyi Ji,^{1,2} Guoliang Yu,^{1,2} Changsong Xu^{1,2,*} and H. J. Xiang^{1,2,3,†}

¹Key Laboratory of Computational Physical Sciences (Ministry of Education), Institute of Computational Physical Sciences, and Department of Physics, Fudan University, Shanghai 200433, China

²Shanghai Qi Zhi Institute, Shanghai 200030, China

³Collaborative Innovation Center of Advanced Microstructures, Nanjing 210093, China

 (Received 19 October 2022; revised 15 January 2023; accepted 15 February 2023; published 4 April 2023)

Two-dimensional (2D) ferroelectrics, which are rare in nature, enable high-density nonvolatile memory with low energy consumption. Here, we propose a theory of bilayer stacking ferroelectricity (BSF), in which two stacked layers of the same 2D material, with different rotation and translation, exhibit ferroelectricity. By performing systematic group theory analysis, we find all the possible BSF in all 80 layer groups (LGs) and discover the rules about the creation and annihilation of symmetries in the bilayer. Our general theory can not only explain all the previous findings (including sliding ferroelectricity), but also provide a new perspective. Interestingly, the direction of the electric polarization of the bilayer could be totally different from that of the single layer. In particular, the bilayer could become ferroelectric after properly stacking two centrosymmetric nonpolar monolayers. By means of first-principles simulations, we predict that the ferroelectricity and thus multiferroicity can be introduced to the prototypical 2D ferromagnetic centrosymmetric material CrI_3 by stacking. Furthermore, we find that the out-of-plane electric polarization in bilayer CrI_3 is interlocked with the in-plane electric polarization, suggesting that the out-of-plane polarization can be manipulated in a deterministic way through the application of an in-plane electric field. The present BSF theory lays a solid foundation for designing a large number of bilayer ferroelectrics and thus colorful platforms for fundamental studies and applications.

DOI: [10.1103/PhysRevLett.130.146801](https://doi.org/10.1103/PhysRevLett.130.146801)

Introduction.—Ferroelectrics are important functional materials and are widely used as sensors, actuators, and information devices. The recent emergence of two-dimensional (2D) ferroelectrics, overcoming the size effects, leads to promising applications of high-density memory [1–3] and new optoelectronic devices [4–6]. So far, the number of experimentally determined 2D ferroelectrics is rather limited. The first example of 2D room-temperature ferroelectrics is CuInP_2S_6 [7–9]. In 2016, SnTe films were synthesized to the limit thickness of one unit cell and exhibited robust in-plane ferroelectricity at nearly room temperature [10]. Later, another ferroelectric monolayer $\alpha\text{-In}_2\text{Se}_3$ was prepared from its van der Waals bulk and was demonstrated to possess both out-of-plane and in-plane polarization. Moreover, an organic-inorganic hybrid ferroelectric BA_2PbCl_4 [11] and a type-II multiferroic, NiI_2 [12] were recently reported. Despite such examples, the limited choices of 2D ferroelectrics strongly hinders fundamental studies and realistic applications.

Recently, sliding ferroelectricity was proposed to construct 2D ferroelectrics from nonferroelectric monolayers. The sliding ferroelectricity refers to the phenomenon that ferroelectricity can arise from a bilayer, which is made of two monolayers, and the polarization can be switched by sliding one monolayer with respect to another. Such an idea was theoretically proposed by Li and Wu in 2017, in the demo

bilayers of BN and MoS_2 [13]. The sliding ferroelectricity in BN was then experimentally observed by two groups in 2021 [14,15]. Furthermore, the sliding ferroelectricity is also realized in bilayers of transition metal dichalcogenides, such as WTe_2 and MoS_2 [16–21]. However, current studies on sliding ferroelectricity are limited to specific systems and peculiar amounts of sliding, leaving a large number of 2D systems unexplored. Hence, a general rule, which can govern the generation of ferroelectricity from stacking two monolayers, is highly desired.

In this Letter, by applying group theory to the 80 layer groups (LGs), we propose a more generalized concept of bilayer stacking ferroelectricity (BSF). Such theory can easily tell whether a bilayer exhibits electric polarization and what operations (e.g., rotation and shifting) are needed, with only the LG of monolayer as input. Particularly, the known sliding ferroelectrics BN , MoS_2 , and WTe_2 can be easily understood within the BSF theory, which predicts additional types of electric polarizations in these systems. Moreover, a ferroelectric bilayer is designed from the centrosymmetric monolayer ferromagnet CrI_3 , thus making the bilayer a ferromagnetic–ferroelectric multiferroic. More interestingly, a deterministic approach to flip out-of-plane BSF with an in-plane electric field is proposed.

Group theory analysis of BSF.—Any 2D material can be regarded as a single layer. The bilayer can be seen as two

single layers with the bottom layer unmoved and the top layer stacked onto the bottom layer [see Fig. 1(a)]. For a single layer with a given LG, different stacking operators may lead to different LGs [see Fig. 1(e) as an example] and thus diverse properties of the bilayer. We will derive the stacking operators that transform the LG of a single layer to that of the bilayer. In this section, we first introduce the four polar types, which is closely related to the symmetry operators. Then we discuss the presence or absence of a certain symmetry in the single layer and the bilayer. Finally, we apply the result of individual symmetry operators to all 80 LGs and figure out the group and polar type of the bilayer.

A space group operator \hat{R} (and the corresponding point group operator R) in a LG G gives a constraint on the polarization of a 2D system. All these constraints altogether determine the allowed polarization in the system. Therefore, the 80 LGs can be classified into four polar types [in-plane

polarization (IP), out-of-plane polarization (OP), combined polarization with both in-plane and out-of-plane components (CP), nonpolar (NP)] (see Sec. 1 of Supplemental Material [22]). After stacking one layer to another layer, the polar type of a 2D system may be changed. In essence, this is because, after stacking, some symmetries are broken and new symmetries may emerge. Let us assume that the single layer S , with the LG $G_S = \{\hat{R}_S\}$ (\hat{R}_S is the symmetry operator of the single layer), is parallel to the xy plane. The top layer S' is obtained by applying the stacking operator $\hat{\tau}_z \hat{O}$ on S . Here, $\hat{\tau}_z$ is a trivial out-of-plane translation operator which does not change the symmetry of the bilayer, and $\hat{O} = \{O|\tau_O\}$ is the transformation operator, where O is the rotational part and τ_O is the in-plane translational part. One can easily see that $\hat{O}\hat{R}_S$ leads to the same bilayer as \hat{O} for any $\hat{R}_S \in G_S$. Hereafter for simplicity we use \hat{O} to represent the solution set $\hat{O}G_S$.

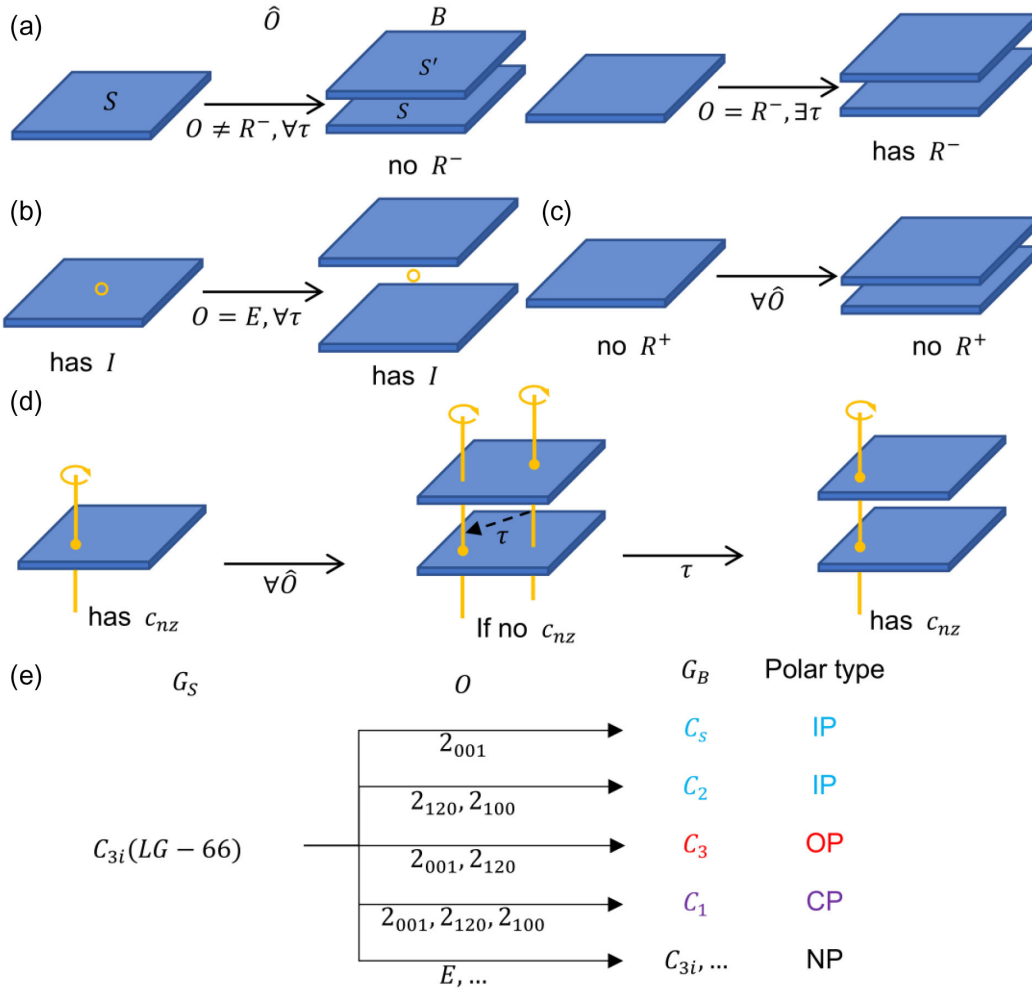


FIG. 1. Schematization of constructing bilayers from monolayers and illustration of the four principles. (a) The R^- symmetry ($I, m_z, c_{2\alpha}, s_{nz}$) can exist in B only if $O \in R^-G_{S0}$. (b) One case of principle (b): pure translation will not break the inversion symmetry. (c) If the single layer does not have $R^+(E, m_\beta, c_{nz})$, the bilayer also does not have this R^+ . (d) A translation that makes two n -fold rotational axes coincide in both layers will preserve the n -fold rotation symmetry. (e) Example of the polar type transformation after bilayer stacking using different rotational operation O . The translational part is omitted here.

The bilayer $B = S + S'$, as shown in Fig. 1(a), with the LG $G_B = \{\hat{R}_B\}$ (\hat{R}_B is the symmetry operator of the bilayer), will satisfy a set of equations due to the presence of symmetries [see Eq. (2) in the Supplemental Material [22]]. If we solve this equation set directly, both G_S, G_B can be one of the 80 LGs and we have to solve 6400 equation sets, which is tedious. More importantly, this direct solving approach may give the final results but will provide not much physical insight. Instead, we propose an alternative easier and physically more appealing approach: (1) we find \hat{O} for a certain point group symmetry operator R_B of the bilayer; (2) we apply the solution about \hat{O} to S with a specific G_S . Since the number of R is about 10 times smaller than the number of G_B , this method is faster than the direct solving approach.

Now let us discuss step (1) of our approach (see Sec. II of the Supplemental Material [22] for details). To solve the equation set, we classify all \hat{R} (\hat{R}_S, \hat{R}_B) of a 2D system into two categories, \hat{R}^\pm . Those R that can (cannot) exchange S and S' are labeled with superscript “-” (“+”), including $\{R^-\} = \{I, m_z, c_{2\alpha}, s_{nz}\}$ ($\{R^+\} = \{E, m_\beta, c_{nz}\}$). Note that the presence of a R^- symmetry leads to a vanishing out-of-plane polarization. We define G_{S0} (G_{B0}) as the point group of the S (B). Considering all R^\pm , we divide the equation sets into four independent cases and solve them separately: (i) $R_B = R^- \in G_{S0}$, (ii) $R_B = R^- \notin G_{S0}$, (iii) $R_B = R^+ \in G_{S0}$, (iv) $R_B = R^+ \notin G_{S0}$. Our theoretical analysis results in several principles [see Figs. 1(a)–1(d)]: (a) The R^- symmetry in the bilayer B must be one of the elements of OG_{S0} , i.e., $R_B^- \in \{R^-\} \cap OG_{S0}$. Thus B has a given R^- symmetry only if $O \in R^-G_{S0}$. In this case, B has no out-of-plane polarization due to the presence of R^- . And one can choose $O \notin R^-G_{S0}$ to ensure the breaking of R^- symmetry and the presence of out-of-plane polarization in B . (b) Any pure

translation $\hat{O} = \{E|\tau_o\}$ (including $\{E|\tau_o\}G_{S0}$) cannot break the inversion symmetry of the single layer, suggesting that sliding ferroelectricity is impossible based on a centrosymmetric single layer. Note that a pure translation τ_o may break all other symmetries. (c) If the bilayer has the R^+ symmetry, such as c_{nz} and m_β , then the original single layer must have the same R^+ symmetry. This indicates that any additional R^+ symmetry cannot be introduced by stacking. (d) For the single layer with the c_{nz} symmetry that excludes the in-plane polarization, whether the c_{nz} symmetry is kept in the bilayer B is determined by the translational part τ_o but not the rotational part O .

These principles are general and suitable for all 2D bilayers, including the twisted bilayers that attracted numerous attentions recently. In 2021, Woods *et al.* observed triangular dipolar domains in marginally twisted hexagonal BN [38]. Recently, Weston *et al.* observed robust room temperature ferroelectricity in marginally twisted MoS₂ [39]. With the present BSF theory, we prove that there is no inversion symmetry in the small angle twisted bilayer and outline two general strategies to construct the CP and IP twisted bilayers [see Sec. 2.3 of Supplemental Material [22]].

As discussed above, twisting provides general strategies to introduce ferroelectricity in the bilayer. However, its large supercell size indicates small electric polarizations. For simplicity and to enhance the electric polarization of the bilayer, we focus on the bilayer that has the same lateral unit cell size as the corresponding single layer. We solve the equation sets and find out how each LG (G_S) of the single layer is transformed into the LG (G_B) of the bilayer under all possible stacking operations $\hat{\tau}_z \hat{O}$. In Table I, we list how the four polar types transform by stacking for all LGs. An example with the LG-66 is shown in Fig. 1(e). Some key

TABLE I. Possible polar types of the bilayer obtained by stacking two monolayers. P_S and P_B denote the monolayer and bilayer polar status, respectively. The labels “√” and “×” represent feasible and infeasible, respectively.

P_S		IP	OP	CP
G_S : LG (PG)		4, 5(C_s), 8 ~ 10(C_2) 27 ~ 36(C_{2v})	3(C_2), 23 ~ 26(C_{2v}), 55, 56(C_{4v}), 77(C_{6v})	49(C_4), 65(C_3) 69, 70(C_{3v}), 73(C_6) 11 ~ 13(C_s)
P_B	IP	√	×	√
	OP	×	√	×
	CP	√	√	√
	NP	√	√	√
P_S		NP		
G_S : LG (PG)		6, 7(C_{2h}), 37 ~ 48(D_{2h}) 61 ~ 64(D_{4h}), 80(D_{6h})	2(C_i), 14 ~ 18(C_{2h}), 19, 21(D_2) 51, 52(C_{4h}), 53, 54(D_4), 57, 58(D_{2d}) 71(D_{3d}), 75(C_{6h}), 76(D_6), 79(D_{3h})	22(D_2), 50(S_4), 59, 60(D_{2d}) 66(C_{3i}), 67, 68(D_3), 72(D_{3d}), 74(C_{3h}), 78(D_{3h})
P_B	IP	×	√	√
	OP	×	×	√
	CP	×	√	√
	NP	√	√	√

findings are summarized: (1) The 2D system that has the same PG (i.e., the highest symmetry with a certain lattice) as its Bravais lattice cannot become ferroelectric through any stacking without expanding the lateral cell size. (2) For other nonpolar systems, it is always possible to introduce in-plane polarization by stacking. (3) If the single layer has in-plane polarization, the stacked bilayer cannot have out-of-plane polarization but vanishing in-plane polarization. (4) Out-of-plane ferroelectricity can be induced by stacking two centrosymmetric monolayers (e.g., the monolayers with C_{3i}).

In the above discussions, we focus on the case where two of the same monolayers are stacked. We find that our BSF theory can be easily adopted to the heterostructure bilayers [see Sec. III of the Supplemental Material [22]] that were recently found to display ferroelectricity [40,41].

BSF in BN and MoS₂.—We apply the above BSF theory to the known sliding ferroelectrics, such as BN, MoS₂, and WTe₂ [see Supplemental Material [22]]. For BN and

MoS₂, it leads to *M* or *N* stacking by simply stacking two monolayers and sliding the top layer by $(1/3, 2/3)$ or $(2/3, 1/3)$, respectively [see Fig. 2(b) and Table S7 in [22] for symmetry points and lines that denote the in-plane translations]. *M* and *N* points have C_{3v} symmetry and out-of-plane polarizations, corresponding to the so-called AB and BA states of the BN bilayer [15]. The bilayer BN and MoS₂ also have possibilities to exhibit pure in-plane polarizations at *A*, *B*, *C* points or along *GA*, *GB*, *GC* lines, and combined polarizations along *GM*, *AN*, *GN*, *BM*, and *MN* lines. These results apply to any systems that share the same LG with BN and MoS₂, e.g., monolayer VGe₂N₄ [36]. Our theory is also applicable to bilayer WTe₂, as detailed in the Supplemental Material [22].

BSF in CrI₃.—We now apply the BSF theory and DFT calculations to CrI₃, which is a typical 2D ferromagnet [42–44]. Monolayer CrI₃ belongs to $p-31m$ (LG-71) and point group of D_{3d} with inversion symmetry. According to Table I, bilayer CrI₃ is possible to form

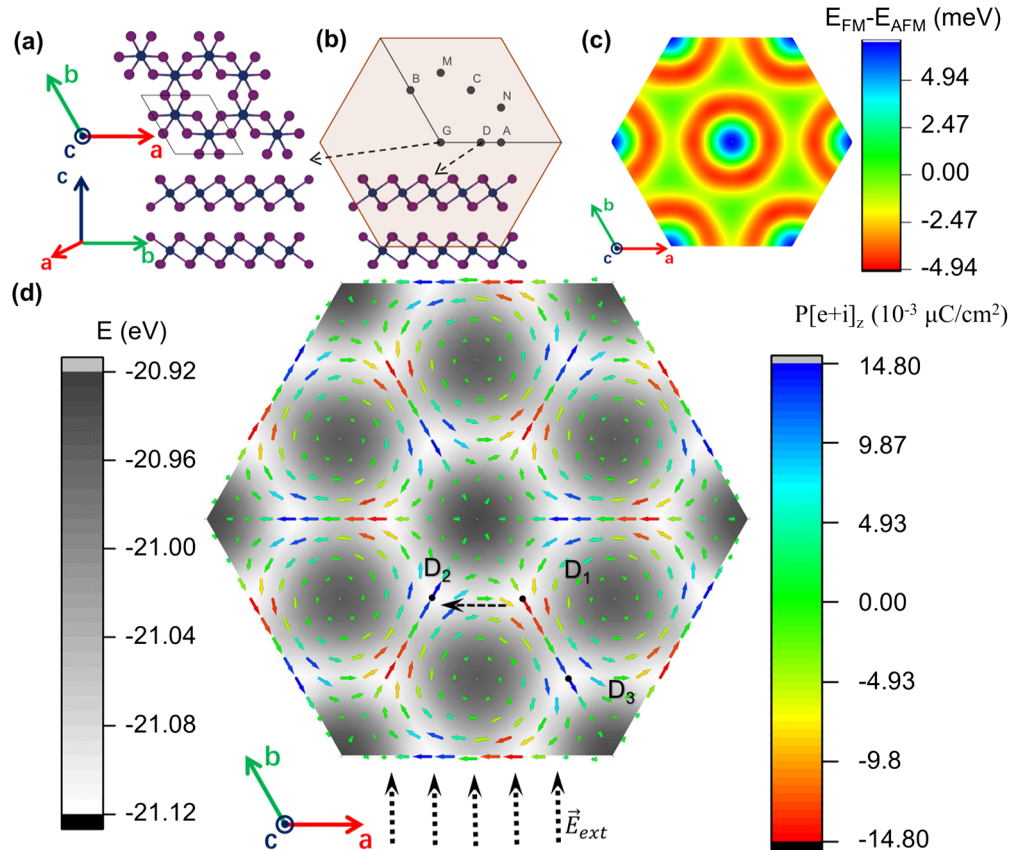


FIG. 2. (a) Top and side views of bilayer CrI₃ obtained using $\hat{O} = \{m_z|0\}$. Purple and blue spheres denote I and Cr atoms, respectively. (b) The six high symmetry translation points in the “unit cell” of τ_0 in the hexagonal crystal system, $G(0, 0)$, $A(1/2, 0)$, $B(0, 1/2)$, $C(1/2, 1/2)$, $M(1/3, 2/3)$, $N(2/3, 1/3)$, the minima point $D(1/3, 0)$ in CrI₃, and side views of bilayer CrI₃ at *D*. The parallelogram with black edges is the “unit cell” of τ_0 . (c) The energy difference between FM and AFM states for different translations. (d) The polarization and energy distribution of the magnetic ground states for different translations. The global ground states around the original point are at $D_{1,2,3...6}: \pm(1/3, 0), \pm(0, 1/3), \pm(1/3, 1/3)$. The in-plane and the out-of-plane polarization components are represented by the solid arrows and its color, respectively. The dotted arrows and dashed arrows show the small in-plane external electric field \vec{E}_{ext} and the corresponding switching pathway, respectively.

the phases that exhibit IP or CP, but not OP. According to Table S7 [22], such states happen in the case that the top layer flips ($O = m_z$), while the simply stacked bilayer exhibits no polarization, due to the maintained inversion symmetry. The phases with IP emerge at A, B, C , as well as along GM, AN, GN, BM, MN , while the states with CP arise along GA, GB, GC . DFT calculations are further performed to identify the energy minima of different stackings and the values of polarizations. As shown in Fig. 2(d), the simply stacked bilayer exhibits no polarization and corresponds to the energy maximum; while shifting the top layer by $\pm 1/3$ along the directions of GA, GB, GC leads to the sixfold degenerate global minima with combined polarizations. The energy gain from maximum to minima yields 47.98 meV/f.u., indicating good stability at minima. The polarization at, e.g., $(1/3, 0)$ point yields $0.1482 \mu\text{C}/\text{cm}^2$, with $0.1475 \mu\text{C}/\text{cm}^2$ in plane and $0.0146 \mu\text{C}/\text{cm}^2$ out of plane. Specifically, the polarizations at GM, AN , and A point toward $[100]$, while those at GN, BM, B point toward $[010]$. Notably, Fig. 2(d) further reveals that it does not have to go across the energy maximum to switch among the ground states. Two types of paths are found to be interesting: (i) $(0, -1/3) \rightarrow (-1/3, -1/3)$, which not only flips the OP component but also rotate the IP component by 120 degrees, and which only needs to overcome a small energy barrier of 6.36 meV/f.u.; (ii) $(1/3, 0) \rightarrow (2/3, 0)$, which only flips the OP component but leaves the IP component unchanged, and which yields a moderate energy barrier of 13.88 meV/f.u. Such results indicate that the BSF theory is well consistent with DFT calculations, and that one has to rely on DFT to identify the polarization values, locate energy minima, and find the suitable transition path.

Moreover, the BSF theory and DFT results also indicate a controllable approach to switch out-of-plane polarization with in-plane electric field. Let us focus on path (i): the direction of IP goes from $[0-10]$ to $[110]$, which indicates that an electric field along $[120]$ (perpendicular to the path, but parallel to the direction of the in-plane polarization difference) is possible to complete such path and that the OP flipping can also be accomplished. Such approach is indeed feasible as that, (i) this path corresponds to the lowest energy barrier and it is the best path to lower the interaction energy with the form of $-E \cdot P$; (ii) that the IP component is about 10 times larger than OP component. Such switching mechanism, which utilizes the locking between in-plane and out-of-plane polarization, is similar to the dipole locking enabled switching in In_2Se_3 [45]. On the other hand, such approach with an in-plane field does not work for path (ii) due to the unchanged IP direction. Note that applying out-of-plane electric field is an uncontrollable way to tune polarization, since each ground state corresponds to three shifting directions, with two degenerate paths (i) and one path (ii). Similarly, it is impossible to switch deterministically the polarization of BN using an

external electric field, as the so-called AB and BA stackings exhibit only out-of-plane polarization and correspond to threefold degenerate switching paths (see Fig. S2 [22]).

The bilayer CrI_3 , at its ground states, is further found to be a rare ferromagnetic and ferroelectric multiferroic system. As revealed by Fig. 2(c), the magnetic ground states yield ferromagnetism at the sixfold degenerate CP states, while the NP states at G, M, N points correspond to antiferromagnetic states. Note that a similarly stacked CrBr_3 bilayer (H-type) with FM state has been prepared [46], indicating a good possibility for the realization of multiferroicity in the presently proposed CrI_3 bilayer. Such ferromagnetic-vs-antiferromagnetic states at different stacking conditions are consistent with previous studies [47–49], and it thus enables multistate storage, together with the presently predicted BSF.

Summary.—To conclude, the BSF theory is proposed to guide the construction of polar bilayers from monolayers. Sliding ferroelectrics are found to be specific cases of the present BSF theory. Combining BSF theory and DFT calculations, the bilayer CrI_3 made of two centrosymmetric monolayers, is predicted to be a ferromagnetic-ferroelectric multiferroic that exhibits both in-plane and out-of-plane polarizations. A novel approach is proposed to flip out-of-plane polarization with in-plane electric field in bilayer CrI_3 .

We acknowledge financial support from the Ministry of Science and Technology of the People’s Republic of China (No. 2022YFA1402901), the support from NSFC (Grants No. 11825403, No. 11991061, No. 12188101, No. 12174060, and No. 12274082), and the Guangdong Major Project of the Basic and Applied Basic Research (Future functional materials under extreme conditions–2021B0301030005). C. X. also acknowledge supports from the open project of Guangdong Provincial Key Laboratory of Magnetoelectric Physics and Devices (No. 2020B1212060030).

*csxu@fudan.edu.cn

†hxiang@fudan.edu.cn

- [1] J. A. Mundy *et al.*, *Nat. Mater.* **16**, 622 (2017).
- [2] V. Garcia and M. Bibes, *Nat. Commun.* **5**, 1 (2014).
- [3] S. Wang, L. Liu, L. Gan, H. Chen, X. Hou, Y. Ding, S. Ma, D. W. Zhang, and P. Zhou, *Nat. Commun.* **12**, 53 (2021).
- [4] D. Yang *et al.*, *Nat. Photonics* **16**, 469 (2022).
- [5] Z.-D. Luo, X. Xia, M.-M. Yang, N. R. Wilson, A. Gruverman, and M. Alexe, *ACS Nano* **14**, 746 (2020).
- [6] L. Lv, F. Zhuge, F. Xie, X. Xiong, Q. Zhang, N. Zhang, Y. Huang, and T. Zhai, *Nat. Commun.* **10**, 3331 (2019).
- [7] A. Belianinov *et al.*, *Nano Lett.* **15**, 3808 (2015).
- [8] F. Liu *et al.*, *Nat. Commun.* **7**, 1 (2016).
- [9] M. Chyashnivyus, M. A. Susner, A. V. Ievlev, E. A. Eliseev, S. V. Kalinin, N. Balke, A. N. Morozovska, M. A. McGuire, and P. Maksymovych, *Appl. Phys. Lett.* **109**, 172901 (2016).
- [10] K. Chang *et al.*, *Science* **353**, 274 (2016).
- [11] L. You *et al.*, *Adv. Mater.* **30**, 1803249 (2018).

- [12] Q. Song *et al.*, *Nature (London)* **602**, 601 (2022).
- [13] L. Li and M. Wu, *ACS Nano* **11**, 6382 (2017).
- [14] K. Yasuda, X. Wang, K. Watanabe, T. Taniguchi, and P. Jarillo-Herrero, *Science* **372**, 1458 (2021).
- [15] M. V. Stern *et al.*, *Science* **372**, 1462 (2021).
- [16] Z. Fei, W. Zhao, T. A. Palomaki, B. Sun, M. K. Miller, Z. Zhao, J. Yan, X. Xu, and D. H. Cobden, *Nature (London)* **560**, 336 (2018).
- [17] Q. Yang, M. Wu, and J. Li, *J. Phys. Chem. Lett.* **9**, 7160 (2018).
- [18] P. Sharma, F.-X. Xiang, D.-F. Shao, D. Zhang, E. Y. Tsymbal, A. R. Hamilton, and J. Seidel, *Sci. Adv.* **5**, eaax5080 (2019).
- [19] J. Xiao *et al.*, *Nat. Phys.* **16**, 1028 (2020).
- [20] X. Wang, K. Yasuda, Y. Zhang, S. Liu, K. Watanabe, T. Taniguchi, J. Hone, L. Fu, and P. Jarillo-Herrero, *Nat. Nanotechnol.* **17**, 367 (2022).
- [21] Y. Wan *et al.*, *Phys. Rev. Lett.* **128**, 067601 (2022).
- [22] See Supplemental Material at <http://link.aps.org/supplemental/10.1103/PhysRevLett.130.146801> for polar layer group and its classification, detailed group theory analysis of BSF, BSF in the bilayer heterostructures, DFT settings, BSF in BN, MoS₂ and WTe₂, DFT results of bilayer stacking BN and NEB barriers and polarization switching for CrI₃ bilayers, which includes Refs. [13,15,17,23–37].
- [23] F. E. Neumann, *Vorlesungen über die Theorie der Elastizität der festen Körper und des Lichtäthers*, edited by O. E. Meyer (B. G. Teubner-Verlag, Leipzig, 1885).
- [24] P. Hohenberg and W. Kohn, *Phys. Rev.* **136**, B864 (1964).
- [25] P. E. Blöchl, *Phys. Rev. B* **50**, 17953 (1994).
- [26] G. Kresse and J. Hafner, *Phys. Rev. B* **47**, 558 (1993).
- [27] G. Kresse and J. Furthmüller, *Comput. Mater. Sci.* **6**, 15 (1996).
- [28] J. P. Perdew, K. Burke, and M. Ernzerhof, *Phys. Rev. Lett.* **77**, 3865 (1996).
- [29] V. I. Anisimov, F. Aryasetiawan, and A. Lichtenstein, *J. Phys. Condens. Matter* **9**, 767 (1997).
- [30] J. Klimeš, D. R. Bowler, and A. Michaelides, *Phys. Rev. B* **83**, 195131 (2011).
- [31] R. Resta, *Ferroelectrics* **136**, 51 (1992).
- [32] R. D. King-Smith and D. Vanderbilt, *Phys. Rev. B* **47**, 1651 (1993).
- [33] R. Resta, *Rev. Mod. Phys.* **66**, 899 (1994).
- [34] G. Henkelman, B. P. Uberuaga, and H. Jónsson, *J. Chem. Phys.* **113**, 9901 (2000).
- [35] G. Henkelman and H. Jónsson, *J. Chem. Phys.* **113**, 9978 (2000).
- [36] Y. Li and Y. Liu, *New J. Phys.* **21**, 083008 (2022).
- [37] K. Yasuda, X. Wang, K. Watanabe, T. Taniguchi, and P. Jarillo-Herrero, *Science* **372**, 1458 (2021).
- [38] C. R. Woods *et al.*, *Nat. Commun.* **12**, 347 (2021).
- [39] A. Weston *et al.*, *Nat. Nanotechnol.* **17**, 390 (2022).
- [40] L. Rogée, L. Wang, Y. Zhang, S. Cai, P. Wang, M. Chhowalla, W. Ji, and S. P. Lau, *Science* **376**, 973 (2022).
- [41] T. Akamatsu *et al.*, *Science* **372**, 68 (2021).
- [42] S. Jiang, L. Li, Z. Wang, K. F. Mak, and J. Shan, *Nat. Nanotechnol.* **13**, 549 (2018).
- [43] B. Huang *et al.*, *Nat. Nanotechnol.* **13**, 544 (2018).
- [44] C. Xu, J. Feng, H. Xiang, and L. Bellaiche, *npj Comput. Mater.* **4**, 57 (2018).
- [45] J. Xiao *et al.*, *Phys. Rev. Lett.* **120**, 227601 (2018).
- [46] W. Chen, Z. Sun, Z. Wang, L. Gu, X. Xu, S. Wu, and C. Gao, *Science* **366**, 983 (2019).
- [47] Y. Jiang, Y. Guo, X. Yan, H. Zeng, L. Lin, and X. Mou, *Nanomater. Nanotechnol.* **11**, 2509 (2021).
- [48] P. Jiang, C. Wang, D. Chen, Z. Zhong, Z. Yuan, Z.-Y. Lu, and W. Ji, *Phys. Rev. B* **99**, 144401 (2019).
- [49] N. Sivasadas, S. Okamoto, X. Xu, C. J. Fennie, and D. Xiao, *Nano Lett.* **18**, 7658 (2018).